Membrane-crystallization of lysozyme

Efrem Curcio, Gianluca Di Profio, Enrico Drioli

Research Institute on Membrane Technology, ITM-CNR,
c/o University of Calabria - Via P. Bucci Cubo 17/C, I-87030 Arcavacata di Rende (CS), Italy

Extended abstract

Protein crystallization plays today a crucial role in the whole field of life sciences. The 3D structure elucidation of bio-macromolecules is essential for an understanding of their complex biological functions. In the pharmaceutical industry, the knowledge of the complete atomic 3D structure is expected to speed up the process of designing new molecules as potential ligands or inhibitors of proteins involved in pathological processes [1-3]. Macromolecular crystallization also represents an important separation/purification step in a number of chemical and biotechnological processes, as well as the first step in the production of cross-linked enzyme crystals (CLECs), with high surface to volume ratio [4]. X-ray crystallography is the method of choice for determining a protein 3D structure at atomic resolution that however requires highly ordered crystals of adequate size ($\geq$ 30-50 μm). Protein crystallization has therefore gained a strategic and commercial relevance in the post-genomic era [5]. In the last few years, there have been some efforts in the development of new practical approaches aiming to improve and to understand the macromolecular crystallization process. Recent advances in methodology for protein crystallization are addressed - with increasing interest - towards the promotion of heterogeneous nucleation, generally induced by charged substrates, polymer-modified surfaces, or exogenous mineral particles [6,7, 8,9,10,11]. Authors have recently proposed an innovative membrane crystallization technique based on the use of microporous hydrophobic polymers [12,13]. Namely, microporous membranes have been used both as the physical support for contacting two liquid isothermal subsystems (protein solution / stripping solution) subjected to mass interchange (solvent extraction from the protein solution) in vapour phase, as well as a synthetic surface able to activate heterogeneous nucleation. The present study aims to investigate both the nucleation and the crystal growth processes of HEWL as result of the interactions occurring between the protein and the polymeric membrane. In particular, kinetic data have been obtained by *in-situ* turbidity analysis, frequently applied as diagnostic tool to monitor the crystal growth process [14] and to measure induction time periods [15].

Lyophilised and three times recrystallized HEWL was used as purchased from Sigma Chemicals Company, without further purification. Stock solutions of sodium chloride in reagent grade (1.0-11.6% wt/v) were prepared in 0.1 M sodium acetate buffer pH 4.6, and used as precipitant; aqueous solutions of magnesium chloride in reagent grade (10-30% wt/v) were used as stripping agent. Solutions of NaCl and lysozyme (initial concentration: 20 mg/mL), both in acetate buffer, were then mixed to give the desired final concentrations of precipitant and protein. Experiments were carried out at 20°C. Hydrophobic microporous polypropylene hollow fibres membranes, with nominal pore size of 0.2 μm and external diameter of 1.8 mm, were wrapped at their bottom and successively arranged in a 2.5 mL quartz cuvette with a path length of 1 cm. The stripping solution was pipetted inside the membrane fibres, whereas the protein/precipitant solution mixture was loaded on the outer part of the membranes. The cuvette was then placed in a UV-Visible spectrophotometer (Perkin Elmer LAMBDA EZ201) thermostated by a POLYSTAT CC1 bath (from Bicasa, Italy); absorbance was recorded automatically at 400 nm every 100 sec for several hours. A video-camera module (Visioscope Modular System) equipped with an optical head 100X was used to monitor protein crystals size. Spectrophotometric measurements of the protein solutions loaded on the membrane crystallization system allowed to obtain the turbidity curves (figure 1): during the time interval (induction period) that precedes the formation of stable crystals nuclei almost no changes in turbidity can be observed.

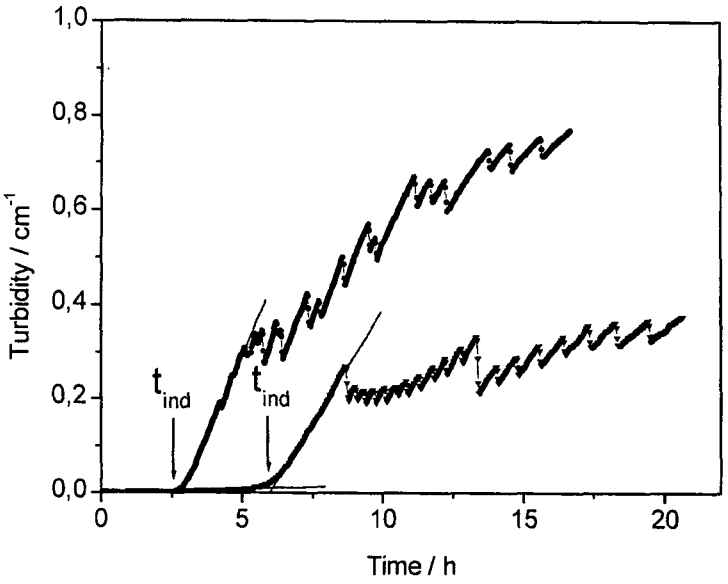

Figure 1. *Typical turbidity profiles obtained during crystallization experiments (HEWL 20 mg/mL in AcNa/AcH buffer, 0.1 M pH 4.6).*

The simultaneous nucleation and growth of protein clusters results in a rapid increase of the turbidity; successive declines are ascribed to crystal sedimentation.
Induction times, measured at different NaCl and $MgCl_2$ concentrations, are comprised between 1.2 and 10 hours (figure 2). At constant NaCl concentration, a decrease of the induction time period is observed when the $MgCl_2$ concentration increases, due to the high rate of solvent extraction.
At a constant $MgCl_2$ concentration, the induction time is reduced by increasing the content of NaCl .

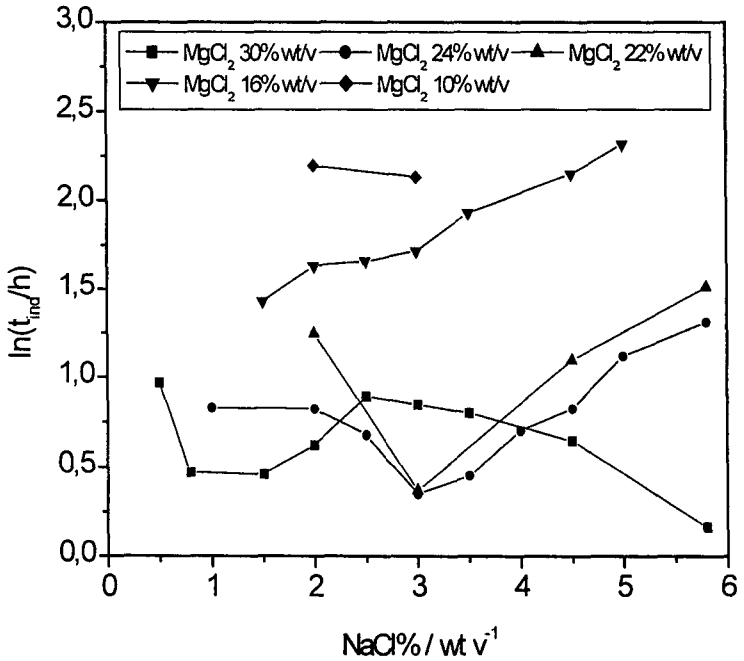

Figure 2. Induction times vs NaCl concentration; $MgCl_2$ % wt/v is indicated in the legend.

However, if the concentration of the precipitant is further increased, the activity gradient between the stripping and the protein/precipitant solutions falls down and leads to a substantial increase in the induction time period. For 16% wt/v $MgCl_2$, an increase of the NaCl concentration from 1.5 to 5% wt/v further reduces the solvent transmembrane flux, and no effect on the protein solubility

consequent to the ionic strength variation is observed. Figure 3 shows the curves of the number of generated nuclei, in the unitary volume, during crystallization trials carried out at 2% wt/v NaCl and at $MgCl_2$ concentrations varying from 16 to 30% wt/v. For each investigated NaCl concentration, an increase in $MgCl_2$ content causes an acceleration of the nucleation rate.

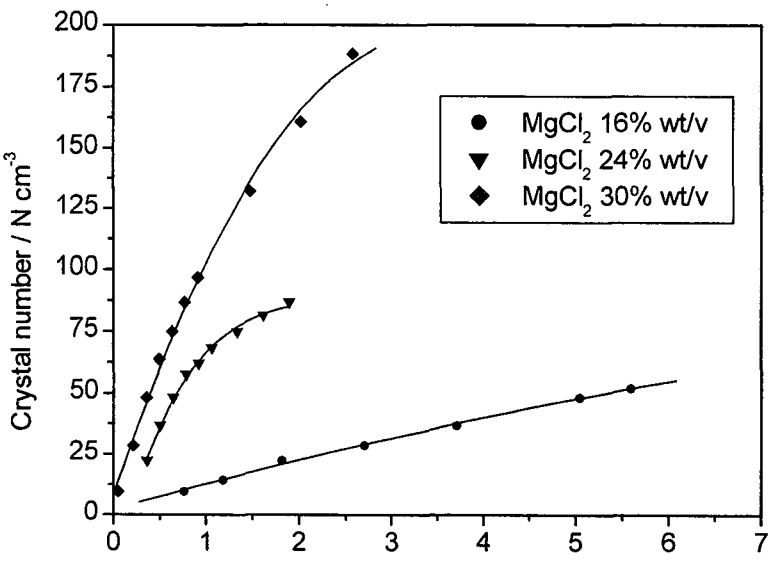

Figure 3. Number of generated crystals at 2% wt/v NaCl, and stripping concentrations reported in the legend

In correspondence of 30% wt/v $MgCl_2$, no significant changes have been observed by varying NaCl concentration in a wide range of values (from 0.8 to 5.8% wt/v); in fact, the high solvent transmembrane flux (activated by an high stripping concentration) allows to rapidly reach supersaturation, therefore making the effect of NaCl irrelevant as precipitant agent. The influence of the NaCl content becomes significant at $MgCl_2$ concentrations below 24% wt/v. High nucleation rates have been measured at low NaCl concentrations due to the reduced protein solution activity that leads to an increase of the solvent transmembrane flux. At 22% wt/v $MgCl_2$, the values of nucleation rate raises when the NaCl content drops from 5.8 to 5% wt/v and lessens when the NaCl concentration decreases from 4.5 to 2% wt/v. An analogous and more evident behaviour has been observed in the case of 16% wt/v $MgCl_2$.

The growth process for crystals of detectable size has been monitored by optical microscopy up to an apparent growth cessation, corresponding to the achievement of a time-invariant mean length. For a stripping concentration of 30% wt/v $MgCl_2$, the initial increase in growth rate due to a NaCl variation from 0.8 to 3% wt/v, is followed by a considerable deceleration when the NaCl concentration is further raised

Lysozyme crystals suitable for diffraction analysis have been obtained at 20°C, 20 mg/mL HEWL, 2% and 2.5% wt/v NaCl, 24% wt/v $MgCl_2$. These experimental conditions allowed to growth crystals with induction time of 2.3 and 2 hrs, respectively. Tetragonal, single crystals of HEWL were mount in 0.5 mm diameter glass capillaries in the presence of mother liquor and sealed with wax. Diffraction data have been collected at 25°C, λ=1.00 Å, oscillation range of 1.0°, at the X-ray diffraction beam line XRD-1 of the Italian synchrotron light laboratory ELETTRA (Trieste, Italy) using a MAR CCD x-ray detector system (Mar USA, Inc.). A short exposure time of 10s was chosen in order to minimize crystals decay due to radiation damage. Data processing was done with DENZO, SCALEPACK and the CCP4 package. Crystal, data collection statistics for the two crystals analysed are reported in Table 1.

		CRYSTAL#1	CRYSTAL#2
Dimensions	Linear (mm)	0.25 x 0.20 x 0.11	0.25 x 0.25 x 0.08
	Volume (mm^3)	5.5×10^{-3}	5×10^{-3}
Space Group	$P\,4_3\,2_1\,2$		
Cell	a (Å)	79.403	79.443
	b (Å)	79.403	79.443
	c (Å)	37.832	37.917
Mosaicity (°)		0.167	0.165
Number of Reflections	Total	33198	33821
	Unique	6653	6563
Number of Images		45	45
Resolution	Overall (Å)	15.6 - 1.91	22.03 - 1.91
	Last Shell (Å)	1.93 - 1.91	1.93 - 1.91
R_{merge}	Overall	0.027	0.024
	Last Shell	0.072	0.079
Completeness	Overall (%)	67.6	67.2
	Last Shell (%)	68.3	72.3
Redundancy		5.0	5.2
$\langle I/\sigma(I)\rangle$	Overall	37.0	36.6
	Last Shell	16.3	16.8
B_{Wilson} ($Å^2$)		20.4	20.0

References

[1] A. Mc Pherson, Crystallization of biological macromolecules, Cold Spring Harbor Laboratory Press, Cold Spring Harbor, 1999.

[2] A. Ducruix, R. Giegè, Crystallization of nucleic acid and proteins. A practical approach, IRL Press/Oxford University Press, Oxford, 1992.

[3] A. Mc Pherson, J. Crystal Growth 110 (1991) 1.

[4] A.L. Margolin, M.A. Navia, Angew. Chem. Int. Ed. 40 (2001) 2204.

[5] N.E. Chayen, Trends in Biotechnology 20 (2002) 98.

[6] A. Mc Pherson, P. Schilchta, Science 230 (1998) 385.

[7] N.E. Chayen, E. Saridakis, R. El-Bahar, Y. Nemirovsky, J. Mol. Biol. 312 (2001) 591.

[8] S. Fermani, G. Falini, M. Minnucci, A. Ripamonti, J. Crystal Growth 224 (2001) 327.

[9] E Pechkova, C. Nicolini, J. Crystal Growth 231 (2001) 599.

[10] L. Rong, H. Komatsu, S. Yoda, J. Crystal Growth 235 (2002) 489.

[11] G. Falini, S. Fermani, G. Conforti, A. Ripamonti, Acta Cryst. D58 (2002) 1649.

[12] E. Curcio, G. Di Profio, E. Drioli, J. Crystal Growth 247 (2002) 166.

[13] E. Curcio, G. Di Profio, E. Drioli, Separation and Purification Technology, *in press*.

[14] L.H. Dao, H.M. Nguyen, H.H. May, ACTA Astronautica 47 (2000) 399.

[15] H. Hu, T. Hale, X. Yang, L.J. Wilson, J. Crystal Growth 232 (2001) 86.